Stimulation-Induced Muscle Deformation Measured With A-Mode Ultrasound Correlates With Muscle Fatigue

Jonathan T. Alvarez, Yichu Jin, Dabin K. Choe, Elizabeth L. Suitor, and Conor J. Walsh

***Abstract*— Muscle fatigue is a common physiological phenomenon whose onset can impair physical performance and increase the risk of injury. Traditional assessments of muscle fatigue are primarily constrained by their dependence on maximum voluntary contractions (MVCs), which not only rely heavily on participant motivation, reducing measurement accuracy, but also require large, stationary equipment such as isokinetic dynamometers, limiting their application to discrete assessments in lab-based environments. In this work, we introduce a wearable muscle fatigue tracking strategy that employs low-profile single-element ultrasound and electrical stimulation. This integrated approach demonstrates that muscle deformation from electrically-induced muscle contractions correlates with muscle fatigue, thus circumventing the need for bulky hardware and eliminating the variability associated with human volition. We define a deformation index, which fuses stimulation-induced changes in muscle thickness with baseline muscle swelling to track muscle fatigue. Our results demonstrate that the deformation index reliably tracks muscle fatigue ($r = 0.85 \pm 0.15$), under specific conditions, namely extended joint angles and increased stimulation, as measured by changes in knee extension torque during a series of dynamic, volitional fatiguing contractions on 8 subjects on an isokinetic dynamometer. This approach has the potential to enable real-time, semi-continuous muscle fatigue monitoring in unconstrained environments.**

***Index Terms*— Muscle fatigue, wearable technology, electrical stimulation, A-mode ultrasound, muscle deformation.**

I. Introduction

MUSCLE fatigue is a complex phenomenon, involving changes in global cortical activation, local neural motor input to muscle, and underlying physiological and metabolic changes to muscle state [1], [2], [3]. The progression of fatigue has significant implications for a variety of application areas including sports, rehabilitation medicine, and occupational health and safety [4]. The most common way to evaluate fatigue is by tracking a participant's ability to perform a certain task over time. For example, participants are often asked to maintain a submaximal torque target for a period of time or perform consecutive maximum voluntary contractions (MVCs) to evaluate the progression of muscle fatigue [5], [6].

While accurate, MVC testing has two key limitations. First, this approach requires some way of measuring muscle force, such as with an isokinetic dynamometer, which limits its use to research or clinical settings [7]. Moreover, these evaluations can only be conducted at discrete intervals, often pre- and post-exercise. A more effective approach would continuously monitor fatigue during dynamic activities to provide targeted and timely feedback. Second, standard protocols for fatigue evaluation are limited by their reliance on MVCs during measurements. Such dependence on volition can introduce variability in results due to differences in individuals' motivation and effort, complicating the interpretation of muscle fatigue levels [8], [9], [10], [11]. MVC testing is also impractical for certain clinical populations, such as patients recovering from surgery who cannot exert maximum force without risking injury [12]. Furthermore, neurological conditions like stroke may lead to central activation deficits, which can prevent full muscle activation during testing, resulting in underestimated muscle strength and ultimately confounding results [13], [14].

In response to the size and portability constraints of traditional muscle fatigue assessment tools, the field often employs systemic measurement approaches such as heart rate monitoring [15], [16], measuring metabolic cost [17], [18], or blood lactate testing [19] that assess physiological responses across the entire body. However, the broad scope of these measures limits their ability to provide specific insights into individual muscles or muscle groups, as they capture global physiological responses rather than localized muscle activity. Targeted and wearable approaches for estimating muscle fatigue do exist, such as surface electromyography (EMG) [20], [21], mechanomyography (MMG) [22], [23], and near-infrared spectroscopy (NIRS) [24], [25], among which EMG is the predominant method [26]. EMG features are commonly

Received 14 July 2024; revised 17 October 2024; accepted 28 November 2024. Date of publication 4 December 2024; date of current version 17 December 2024. This work was supported in part by the Harvard Move Laboratory and in part by the Harvard John A. Paulson School of Engineering and Applied Sciences. The work of Elizabeth L. Suitor was supported by the National Science Foundation under Grant #DGE2140743. *(Jonathan T. Alvarez, Yichu Jin, and Dabin K. Choe contributed equally to this work.) (Corresponding author: Jonathan T. Alvarez.)*

This work involved human subjects or animals in its research. Approval of all ethical and experimental procedures and protocols was granted by the Harvard Medical School Institutional Review Board under Application No. IRB 17-1201.

The authors are with the John A. Paulson School of Engineering and Applied Sciences, Harvard University, Boston, MA 02134 USA (e-mail: jonathanalvarez@g.harvard.edu; walsh@seas.harvard.edu).

Digital Object Identifier 10.1109/TNSRE.2024.3511267

used to estimate fatigue in clinical diagnostics, sports science, and rehabilitation [21]. Specifically, changes in the median frequency (MDF) and root-mean-square (RMS) voltage of an EMG signal can be tracked to monitor the progression of fatigue [26], [27]. However, despite its utility, EMG has several limitations that complicate its interpretation [28], [29]. These include cross talk from adjacent muscles, interindividual physiological differences, and interfacial variability, such as changes in electrode-skin impedance caused by sweating. Moreover, the interpretation of EMG during dynamic activities faces additional challenges due to the influence of muscle velocity and length on the relationship between the electrical and mechanical activity of muscle [30].

Researchers have investigated how muscle deformation can be used as a marker of muscle force and, by extension, fatigue. As a muscle contracts, it shortens along its longitudinal axis, bulging outwards and changing in thickness and width, architectural changes which have been shown to correlate with muscle force [31], [32], [33]. Traditional brightness mode (B-Mode) ultrasound, with its ability to capture detailed muscle architecture, has been used to understand the progression of muscle fatigue by tracking thickness changes over time [34], [35], [36]. However, due to the challenge of reliably extracting architectural parameters from B-Mode images, most fatigue research with B-Mode ultrasound derives meta-parameters from collected images, such as echogenicity [37], [38], [39], muscle contractility [40], [41], [42], or textural entropy [43] to correlate with fatigue, rather than deformation [44]. While B-Mode ultrasound can offer detailed insights into muscle architecture, the widespread adoption of B-Mode ultrasound beyond research settings is still limited by its significant hardware and computational complexity [26]. Amplitude mode (A-mode) ultrasound has emerged as a potential wearable alternative to B-Mode, promising real-time, muscle-specific measurements for a fraction of the hardware and computational demands [45], [46], [47]. A-mode ultrasound uses single-element transducers (SETs) to track one-dimensional (1D) changes in muscle (e.g., thickness). It has also shown promise in the estimation of static and dynamic muscle force [48], [49] and classification of various kinematic poses [50]. Regarding fatigue, three studies have explored the use of A-mode ultrasound for muscle fatigue monitoring during strenuous, volitional activity: one study categorized muscle states [51], while the other two tracked muscle thickness during a single submaximal hold [52], [53]. However, despite the opportunity and promise of A-Mode ultrasound for real-time, muscle-specific measures of fatigue, A-Mode ultrasound alone does not address the second major limitation of traditional fatigue evaluation—its reliance on MVC testing.

To overcome the variability introduced by participant effort in fatigue evaluation, researchers have turned to electrical stimulation (ES) to directly activate muscle fibers, bypassing the central nervous system altogether. When paired with force measurement tools, ES has been shown to enable precise and accurate measurement of a muscle's force-generating capacity over time, mitigating the variability associated with voluntary effort [2], [3], [54], [55]. However, the precision ES can bring to muscle fatigue assessment is still constrained by the inherent dependence on external force measurement devices, which has historically restricted its use to clinical or research settings. Tensiomyography (TMG) offers an alternative ES-based method for estimating fatigue by measuring radial muscle belly displacement in response to electrical stimulation, thus providing an indirect measure of muscle force without the need for direct force or torque measurements [11], [56], [57]. While TMG illustrates how ES can be used to assess fatigue without direct force measurement, it is limited to benchtop use, requiring a linear displacement sensor to measure radial displacement. In response, ES has more recently been paired directly with wearable methods, such as MMG, enabling more accessible and continuous muscle function monitoring. While traditional EMG is incompatible with ES without significant processing or specialized hardware [58], MMG has been used synchronously with ES to track fatigue [59]. However, MMG is restricted to superficial muscles and is susceptible to crosstalk issues from adjacent muscles like EMG [27], [60]. A-Mode ultrasound is also compatible with ES, and researchers have demonstrated their combined use for monitoring changes in muscle thickness during fatigue induced by repetitive electrical stimulation, but not during volitional exercise [46], [47].

The objective of this study was to assess the simultaneous use of electrical stimulation and wearable A-mode ultrasound to semi-continuously monitor changes in muscle force generation during a volitional dynamic fatiguing activity. Using electrical stimulation to directly activate resting muscles, we explored how stimulation-induced changes in muscle deformation, measured via A-Mode ultrasound, could serve as indicators to estimate simultaneously generated torque and track deficits in overall volitional MVCs.

II. Methods

A. Measurement Devices

1) Amplitude-Mode Ultrasound: Four 5 MHz SETs (Alpha 113-124-660, Waygate Technologies, Germany) were mounted in a custom 3D printed case (35 mm by 43 mm) at angles of 0°, 1.25°, 2.5°, and 3.75°. These transducers were worn on the upper thigh using a compression band (Scosche, USA). Thin layers of ultrasound gel (Aquasonic, USA) were applied to the SETs before donning. The transducer assembly had a total mass of 35.1 g (excluding the transducer cables). Raw radio-frequency data of the four SETs was collected using a portable ultrasound engine (Ursus Medical, Pittsburgh, PA) with custom software (Brodware). Each SET had a frame rate of 100 Hz. The receiver recorded echoes up to a depth of 80 mm with sampling frequency set to 40 MHz. 1540 m/s was used as the speed of sound in human tissues (Fig. 1). To account for human variability, we selected the SET with the strongest echo intensity among the four for further processing, extracting changes in muscle thickness using a muscle boundary tracking algorithm previously outlined in [49].

2) Electrical Stimulation (ES): A current-controlled stimulator (Rehamove3, Hasomed, Germany) delivered biphasic symmetric electrical stimulation to 3 by 5 inch electrodes

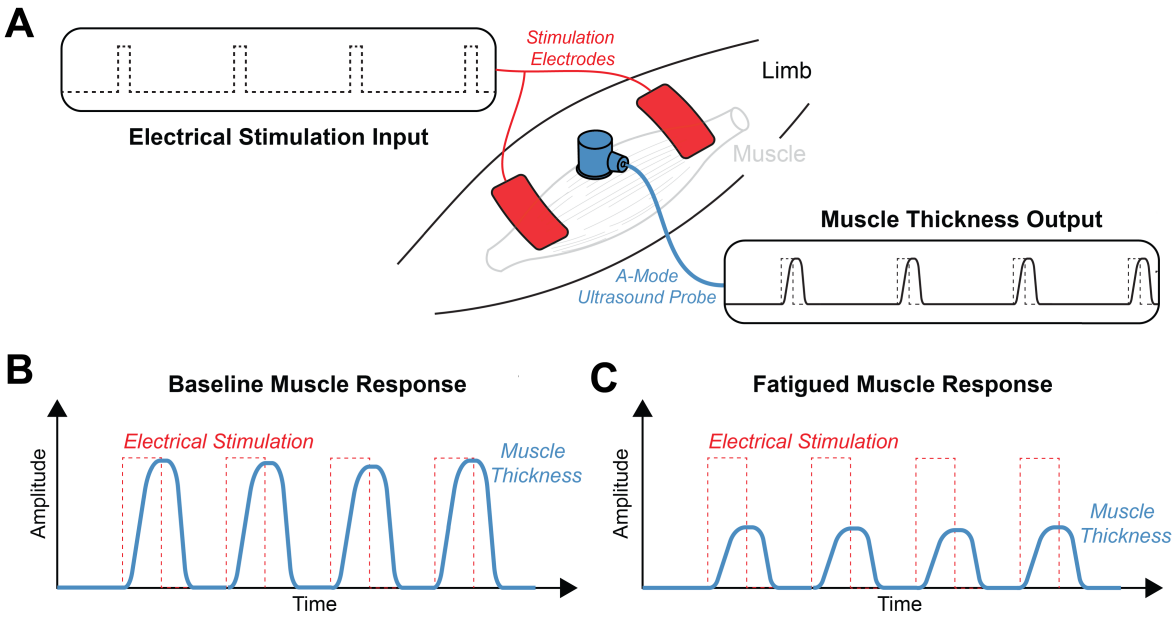

Fig. 1. Overview of the combined stimulation and deformation sensing methodology. (A) Electrical stimulation directly induces a muscle contraction. Simultaneously, a single-element transducer measures A-Mode ultrasound data to derive muscle thickness. By monitoring changes in thickness in (B) baseline (unfatigued) and (C) fatigued muscle in response to targeted electrical stimulation, muscle fatigue can be estimated.

placed distally and proximally to the muscle belly of the rectus femoris (RF). Two types of stimulation were used in this study, twitch and train pulses. Both twitch and train stimulations were used to compare the levels of stimulation required to detect fatigue. A twitch pulse refers to a single pulse and reflects the muscle's response to a single stimulus, typically activating a small number of motor units. A train pulse refers to a pulse train, which is generated by chaining single pulses at a fixed frequency over a designated train duration period leading to the recruitment of multiple motor units. Both types of stimulation were tested to determine the minimum amount of stimulation necessary for reliable fatigue detection. Stimulation parameters for the present study were adapted from [61]. The current amplitude for both stimulus types was fixed at 90 mA. For the train stimulus, the pulse train frequency was fixed at 30 Hz and the train duration was fixed at 250 ms. Individual stimulus pulse duration was determined per participant as outlined in the experimental protocol. To ensure targeted muscle activation, pulse duration was chosen as the minimum required to reach the specified torque target [62].

3) Electromyography (EMG): Two bipolar surface EMG electrodes (Ultium, Noraxon, USA) were placed on the RF to measure electrical activity during the protocol. Electrodes were placed following SENIAM recommendations for each of the target muscles [63]. Raw EMG data were sampled at 2 kHz and filtered through a two-stage filtering approach [64]. First, data were high-pass filtered using a 3rd-order Butterworth filter with a 20 Hz cutoff to attenuate low-frequency noise and stabilize baseline drift. Second, a low-pass Butterworth filter with a 500 Hz cutoff was applied to reduce high-frequency components.

4) Isokinetic Dynamometer: All experiments were conducted on an isokinetic dynamometer (HUMAC Norm, CSMi Solutions, USA), which served as a ground truth measure of joint torque. Isokinetic dynamometers are capable of measuring torque during isometric (fixed-angle) and isokinetic (fixed-velocity) contractions. All torque data were low-pass filtered with a 4th-order Butterworth filter with a 150 Hz cutoff.

5) Data Acquisition Unit: All data were synchronized through a PowerLab 8/35 external data acquisition unit (AD Instruments, New Zealand) sampling at 10 kHz. This unit logged torque and position via analog outputs from the dynamometer. Synchronization 5V pulses emitted by the EMG, ES, and ultrasound systems were also logged and used to align all data in post-processing.

B. Experimental Protocol

The experimental protocol was designed to assess the effects of fatigue on both volitional and stimulation-generated joint torque, ultrasound-derived muscle deformation, and EMG-measured neuromuscular activity (Fig. 2).

Eight healthy participants, (six males, two females; mean±SD: 28.3±1.8 years; height: 1.77±0.07 m; mass: 69.1±13.8 kg) were recruited to participate in this study. All participants self-reported as active individuals. For all participants, the right leg was tested on, regardless of dominance. All participants provided written informed consent before participation. The study was approved by the Harvard Medical School Institutional Review Board (IRB 17-1201).

Prior to testing, participants were led through a series of static and dynamic warm-up stretches. Following the warm-up, participants were instructed to mount the dynamometer, placed in an upright sitting position, and secured to the chair with chest and waist straps to minimize compensatory trunk movements during contractions. A standardized calibration

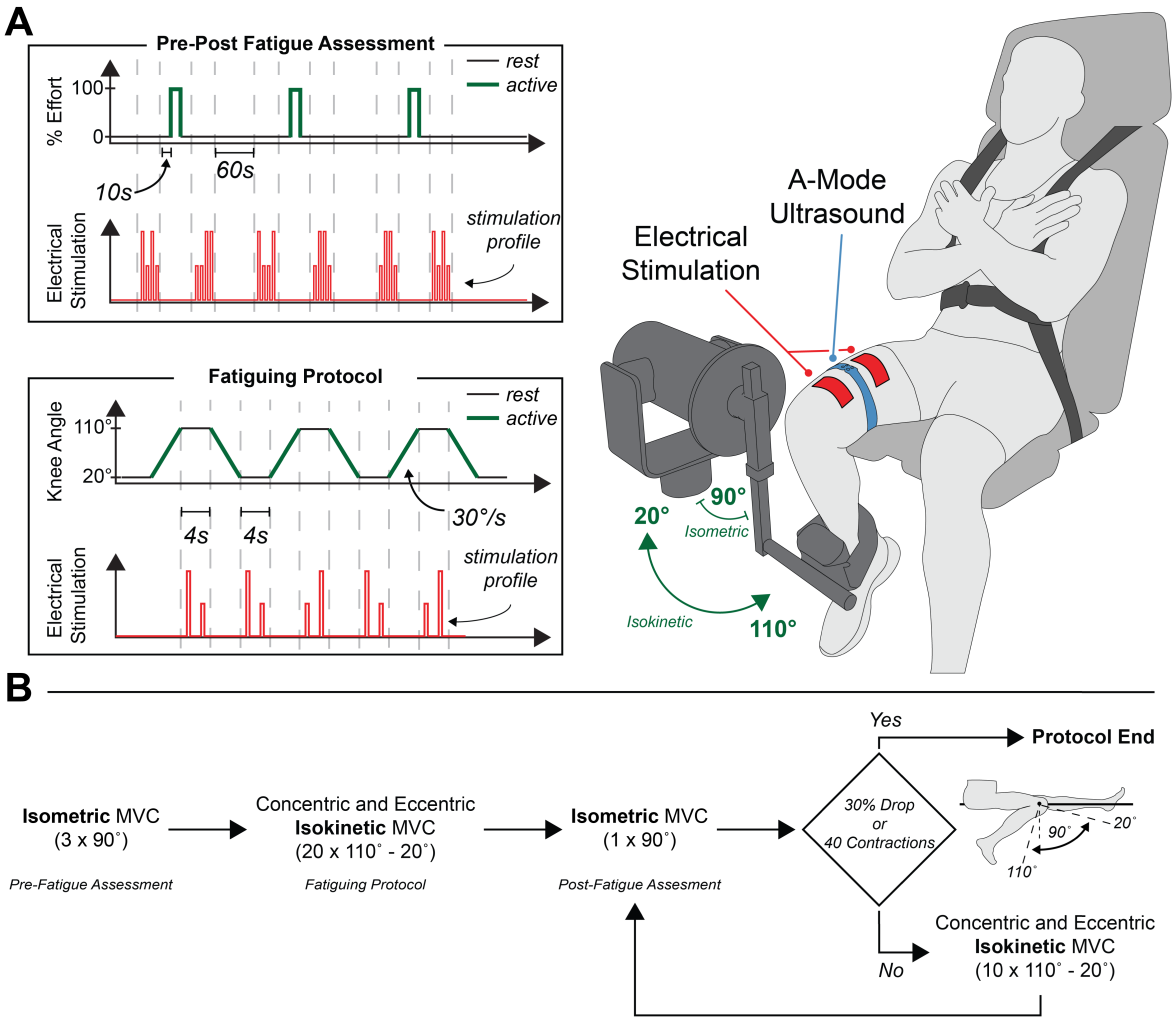

Fig. 2. Overview of the experimental protocol. (A) Illustration of the experimental protocol timing schedule for volitional and stimulated contractions. (B) All participants first performed three maximum effort volitional isometric contractions (MVIC). Before and after each contraction, two twitch and two train pulses were delivered to resting muscle, in random order. The fatiguing protocol which followed consisted of a minimum of 20 maximum concentric and eccentric knee extension contractions. At each end of the range of motion, the dynamometer was locked, and one twitch and one train pulse was delivered to the resting muscle, in random order. Following the completion of the fatiguing protocol, a single MVIC was performed, with resting stimulation delivered before and after the MVIC.

procedure was performed to establish the participant's knee range of motion (ROM) between extended 20° and flexed 110° knee angles. All testing in this study was conducted during knee extension movements, with 0° defined as full knee extension (Fig. 2A). With the participant set up in the dynamometer, the transducer assembly containing the four SETs was then placed above the muscle belly of the RF. Following initial placement, participants were instructed to perform several isometric knee extension contractions, during which the motion mode (M-Mode) ultrasound signal was monitored by the researchers. The position of the transducer assembly was adjusted until the muscle boundaries captured by each SET were visible throughout the full contraction range. Next, the two electrical stimulation electrodes were adhered just distal and proximal of the transducer assembly, centered along the longitudinal axis of the RF. Finally, the two bipolar EMG electrodes were adhered over the RF. Following placement of the transducers, stimulation electrodes, and EMG electrodes, participants were instructed to perform a set of submaximal isometric and isokinetic knee extension contractions to familiarize themselves with the contraction types.

Next, participants were asked to perform a single maximum voluntary isometric contraction (MVIC) at a neutral knee angle of 90° to both potentiate the knee extensors [65] as well as serve as a torque threshold for subsequent stimulation calibration. Whenever participants were asked to perform a "maximal" contraction, they were verbally encouraged by the research staff. For maximal dynamic contractions, participants were instructed to generate maximal force throughout the entire range of motion. To calibrate stimulation parameters, a fixed-amplitude biphasic train (90 mA, 30 Hz, 250 ms) was delivered to the resting muscle. The pulse duration was individualized for each participant and gradually increased until the stimulation generated 10% of the potentiated MVIC contraction torque, with the knee maintained at a fixed 90° angle under isometric conditions.

The main experimental protocol was divided into three sections: a pre-fatigue assessment, a fatiguing protocol, and a post-fatigue assessment (Fig. 2B).

1) Pre-Fatigue Assessment: Participants were asked to perform a series of three MVICs at a neutral knee angle of 90° (Fig. 2B). Before and after each MVIC, participants received four resting stimulations (when the muscle was relaxed), consisting of two twitch and two train pulses, presented in random order (Fig. 2A). Each set of MVICs was separated by a 60 second recovery period to minimize fatigue. The highest torque generated during the three MVICs was recorded as the MVIC value for each participant. Data from this single contraction was then used for comparison with the post-fatigue contraction (Fig. 2B).

2) Fatiguing Protocol: The fatiguing protocol was designed to induce a reduction in peak isometric torque by fatiguing the quadriceps muscles through a series of maximum effort isokinetic concentric and eccentric knee extension contractions. Following each contraction, resting stimulation was administered to the participants (Fig. 2A). The fatiguing protocol consisted of a set of "interrupted isokinetic contractions" repeated a fixed number of times (Fig. 2B). Each set consisted of a four-part sequence, beginning with a maximal effort isokinetic concentric knee extension contraction, moving from a knee angle of 110° to 20° at an angular velocity of 30°/s. Upon reaching a knee angle of 20°, the dynamometer locked for four seconds. During this period, participants were instructed to relax completely, at which point one twitch and one train pulse were administered to the resting muscle, in random order. The sequence continued with a maximal effort eccentric knee extension contraction moving back from 20° to 110° at an angular velocity of 30°/s. Once more, upon reaching 110°, the dynamometer was locked in place for four seconds, participants were instructed to relax completely, and one twitch and one train pulse were delivered to resting muscle, in random order. Following the completion of 20 interrupted isokinetic contractions, the dynamometer was locked at a knee angle of 90° and participants began the post-fatigue assessment (see below). If their peak MVIC torque had decreased by 30% relative to their pre-fatigue MVIC torque the protocol concluded. However, if the reduction in the participant's peak MVIC torque did not meet the 30% threshold, participants continued with up to two additional sets of 10 interrupted isokinetic contractions, until either the 30% reduction in peak isometric torque was reached or a total of 40 sets had been completed. The early stopping criteria of a 30% reduction in MVIC torque was included to prevent excessive fatigue in participants.

3) Post-Fatigue Assessment: The post-fatigue assessment consisted of one MVIC, preceded and followed by four resting stimulations (two twitch, two train; randomized) performed immediately after the fatiguing protocol. Note, if the fatiguing protocol ended because the participant's peak torque had decreased by 30% relative to their pre-fatigue MVIC, two-thirds of the post-fatigue assessment had already been completed, and only the final resting stimulations remained to be administered.

C. Outcome Metrics

1) Deformation Index: When stimulated, the knee extensors deform in width and thickness. This deformation was quantified using a new metric, the deformation index. Derived from A-Mode data, the deformation index was computed by calculating the maximum induced deformation per stimulated contraction (ΔMT) and normalizing it by the resting muscle thickness at the time of stimulation delivery (MT_0) (Fig. 3C). The deformation index was designed to capture the combined effect of changing muscle contractility and swelling during fatigue [3], [11], [66]. Across the entire experimental protocol, the deformation index was calculated per twitch and train stimulation for each participant (Fig. 3B).

2) Voluntary and Stimulated Torque: From the pre-fatigue assessment, the maximum voluntary torque generated across the three MVICs was recorded (Fig. 3D) [67]. The stimulation-generated peak torque was then recorded per twitch and train stimulation before and after the maximum contraction identified from the three MVICs (Fig. 3A). Maximum voluntary and stimulated torque were similarly recorded from the post-fatigue assessment [3]. From the fatiguing protocol the maximum voluntary isokinetic torque per concentric and eccentric contraction were calculated.

3) EMG Median Frequency and Root-Mean Square Voltage: EMG median frequency (MDF) and root-mean-square (RMS) voltage were calculated for all voluntary contractions. For both the pre- and post-fatigue assessments, MDF and RMS values were determined within a 600 ms window centered around the maximum force generated during each isometric contraction. During the fatiguing protocol, MDF and RMS were assessed separately for concentric and eccentric isokinetic contractions. For each contraction phase, EMG MDF and RMS were calculated from data starting 250 ms after movement onset and continuing up until 250 ms before the range of motion limit was reached.

D. Results Processing and Statistical Analysis

1) Pre- and Post-Fatigue Assessment: For the pre- and post-fatigue assessment, a paired t-test was used to assess the presence of significant differences between each metric before and after fatigue. The Anderson-Darling test was used to assess data normality, and a Johnson transformation was applied to non-normal data.

2) Fatiguing Protocol: To assess the correlation between stimulated torque and the deformation index during the fatiguing protocol, Pearson's linear correlation coefficient was calculated for each stimulation type (twitch or train) and knee angle (20° or 110°) per participant, and reported as mean±standard deviation (mean±SD). Although fatigue is often characterized as a nonlinear phenomenon, linear correlations were used in this work because the focus was on the relationship between torque and the ultrasound-derived deformation index, which was hypothesized to be linear. Pearson's was chosen because it preserves the directionality of the relationship, distinguishing between positive and negative correlations, which is essential for accurately interpreting physiological changes, such as increases or decreases in muscle thickness with fatigue. A linear mixed-effects model was used to examine the influence of joint angle and stimulation type on the correlation between stimulated torque and the deformation index. Participant ID was included

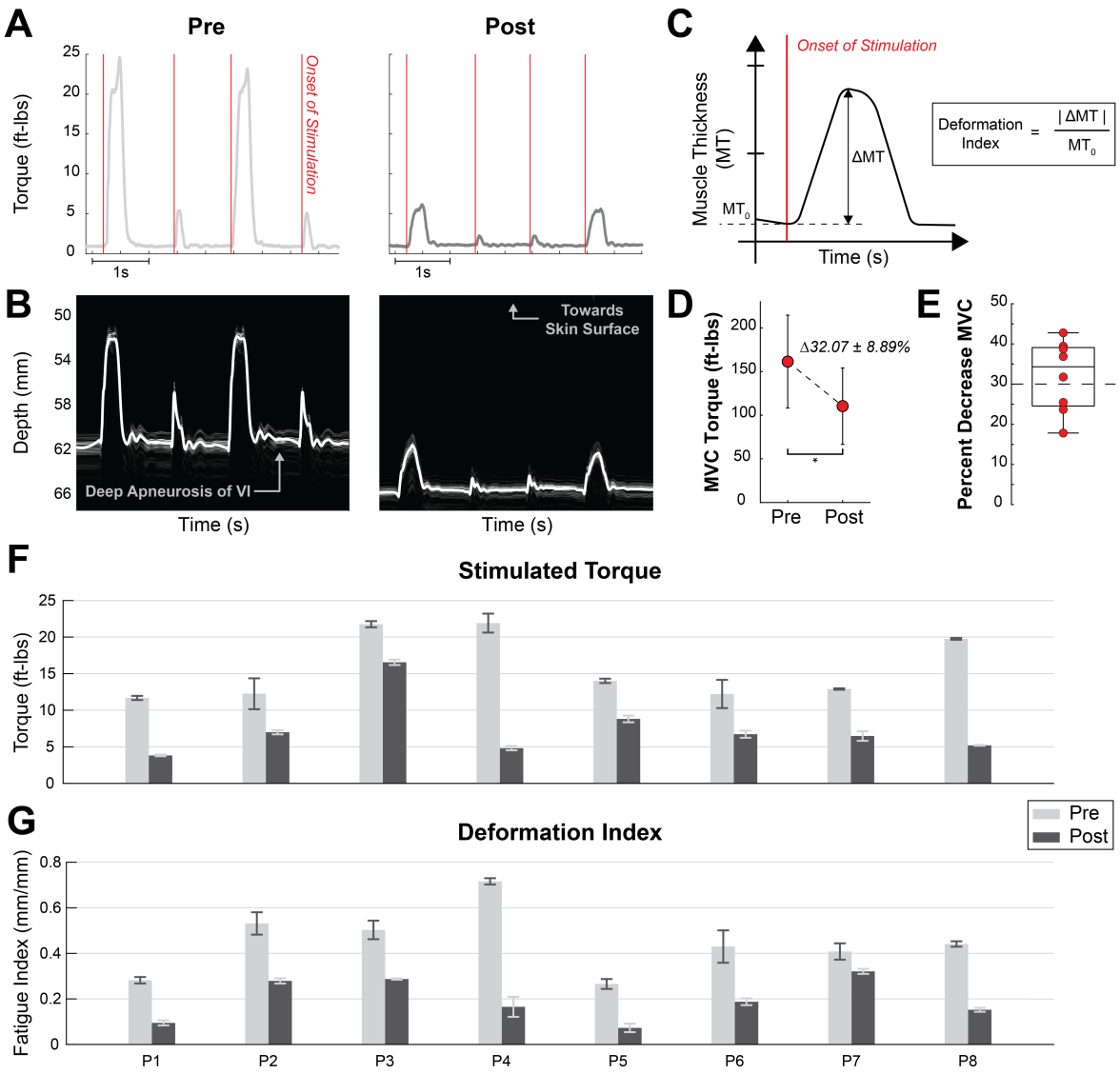

Fig. 3. Overview of data processing and pre-post evaluation results. (A) Stimulated torque response to train and twitch stimulation before and after fatigue, with accompanying (B) M-Mode visualization of muscle thickness. (C) Overview of deformation index metric derivation. ΔMT was calculated as the total range of deformation induced by a single stimulation. MT_0 was defined as the thickness when stimulation was delivered. The deformation index normalizes ΔMT by MT_0. (D) Mean maximum voluntary isometric torque generated by participants before and after fatigue, shown in (E) as a percentage change from baseline. Group-level results showing mean (F) stimulated torque and mean (G) deformation index before and after fatigue across all 8 participants. *Indicates statistically significant mean difference between conditions (determined via paired t-test, $p < 0.05$).

as a random effect, and stimulation type and joint angle were incorporated as fixed effects. Data normality was assessed using the Anderson-Darling test, and through normal probability plots, conditional fits, histograms, and order fit plots. When data were found to deviate from normality, a Johnson transformation was applied to normalize the data. Prior to calculating the correlation coefficients, a Hampel filter with a sliding window of five contractions and a threshold of three standard deviations above the local median was used to detect and remove common outliers [68]. The Hampel filter specifically targeted outliers in the measurements of stimulation-induced deformation and baseline thickness (Fig. 3C) and removed outliers caused either by motion artifacts or inadequate relaxation during the four second rest periods at each end of the range of motion. On average, the Hampel filter identified 7.2% of contractions as outliers, corresponding to approximately 1.4 outliers identified per 20 contractions.

To assess the correlation between volitional torque and EMG MDF and RMS, Pearson's linear correlation coefficient was calculated between peak concentric or eccentric torque and each EMG metric per participant and reported as mean±SD.

Additionally, trends over time across eight participants were examined to compare the consistency in trends of volitionally-generated (concentric and eccentric) versus stimulated (twitch at 20°, train at 20°, twitch at 110°, train at 110°) torque using the Mann-Kendall test. The Mann-Kendall test is a non-parametric method for detecting monotonic trends. In this work, the test was used to identify significant trends in the data, which would indicate a consistent decrease in torque measurements over time [69], reflecting a reliable pattern of

TABLE I
MEAN DIFFERENCES BEFORE AND AFTER THE FATIGUING PROTOCOL

Metric	*Type*	*Percent Decrease (%)*	*Significance*
Volitional Torque	Volitional	-32.1	$p < 0.01$
EMG MDF	Volitional	5.13	$p > 0.05$
EMG RMS	Volitional	-56.6	$p < 0.01$
Stimulated Torque	Train	-52.2	$p < 0.01$
Stimulated Torque	Twitch	-63.2	$p < 0.01$
Deformation Index	Train	-56.2	$p < 0.01$
Deformation Index	Twitch	-56.9	$p < 0.01$

TABLE II
MANN-KENDALL P-VALUES (p_{MK}) DURING THE FATIGUING PROTOCOL

	Volitional Torque		**Stimulated Torque**			
	Conc. Torque	*Ecc. Torque*	*Twitch 20°*	*Train 20°*	*Twitch 110°*	*Train 110°*
P1	**0.010**	**0.0381**	<0.001	<0.001	<0.001	<0.001
P2	**0.042**	<0.01	<0.01	<0.01	<0.001	<0.001
P3	<0.001	**0.112**	<0.01	<0.01	<0.01	<0.01
P4	**0.681**	**0.905**	<0.001	<0.001	<0.001	<0.001
P5	<0.001	<0.01	<0.001	<0.001	<0.001	<0.01
P6	<0.01	<0.01	<0.001	<0.001	<0.001	<0.001
P7	**0.017**	**0.059**	**0.064**	**0.081**	<0.001	<0.001
P8	**0.547**	**0.030**	<0.001	<0.001	<0.001	<0.001

muscle fatigue throughout the testing period. To enhance the robustness of our findings and reduce the likelihood of false positives, we have adopted a more stringent significance level of 0.01 for the Mann-Kendall test results, ensuring greater confidence in detecting true trends.

III. RESULTS

A. Pre- and Post-Fatigue Assessment

All metrics, except for EMG MDF, were significantly influenced by fatigue (Table I). Following the fatiguing protocol, maximum voluntary isometric torque exhibited a significant reduction, decreasing by 32.1% ($p < 0.01$). Similarly, EMG RMS values measured during these contractions also decreased significantly by 56.6% ($p < 0.01$), whereas changes in EMG MDF were not statistically significant ($p > 0.05$). The maximum torque output from both train and twitch stimulations also showed a significant decline following fatigue, decreasing by 63.2% for twitch and 52.2% for train stimulations ($p < 0.01$) (Fig. 3F). The corresponding ultrasound-derived deformation index was also significantly reduced by 56.9% for twitch and 56.2% for train stimulations ($p < 0.01$) (Fig. 3G). Of note, in the pre-fatigue assessment, train stimulation generated 59.2±23.8% more torque and 47.1±13.4% more thickness change (ΔMT) than twitch stimulation on average.

B. Fatiguing Protocol

1) Correlations Between Stimulated Torque and Deformation Index: Across all knee angles and stimulation types, the correlation between stimulated torque and the deformation index during the fatiguing protocol was $r = 0.50\pm0.54$, indicating moderate agreement with significant variability. However, the linear mixed-effects model revealed a significant effect of knee angle ($p < 0.01$) on this correlation; increasing significantly from $r = 0.22\pm0.56$ at 20° to $r = 0.79\pm0.33$ at 110° (Fig. 4C). In contrast, stimulation type alone did not significantly affect the correlation ($p > 0.05$), with twitch and train stimulations showing correlations of $r = 0.46\pm0.57$ and $r = 0.54\pm0.52$, respectively (Fig. 4C). Additionally, the interaction between stimulation type and knee angle did not significantly influence the correlation ($p > 0.05$), indicating that the effect of stimulation type on the correlation between stimulated torque and deformation index is consistent across different knee angles. Overall, the strongest correlation was observed at a knee angle of 110° with train stimulation ($r = 0.85\pm0.15$) (Fig. 4D).

2) Correlations Between Volitional Torque and EMG Metrics: The correlation between volitional torque and EMG metrics during the fatiguing protocol varied significantly depending on the contraction type. For EMG MDF, the correlation during eccentric contractions was low ($r = 0.02\pm0.31$), but increased during concentric contractions ($r = 0.29\pm0.35$). The correlation for EMG RMS demonstrated a moderate association with volitional torque during eccentric ($r = 0.61\pm0.32$) and concentric contractions ($r = 0.56\pm0.3$).

3) Consistency in Trends of Volitional Vs. Stimulated Torque: The Mann-Kendall trend results for the volitional concentric and eccentric MVC torque were mixed, reflecting significant interparticipant variability (Table II). Both concentric and eccentric torque only revealed significant trends ($p_{MK} < 0.01$) in two of the eight participants, with p-values indicating mixed, or weak to no significance in the remaining six participants (shaded red in Table II; $p_{MK} \geq 0.01$). Contrastingly, stimulated torque measurements exhibited strong and consistent negative trends, indicating a reliable decrease in torque values across the testing period (Table II). Seven of eight participants showed highly significant trends for both stimulated twitch and train contractions at 20°. At 110°, all eight participants had consistently significant trends for both stimulation types among the participants.

4) Trends of Stimulation-Induced Thickness Change: At 20°, the knee extensor compartment increased in thickness (normal to the skin surface) in response to stimulation for all participants; however, at 110°, it decreased in thickness for seven out of eight participants when stimulated. For both train and twitch stimulations, the induced deformation (ΔMT) was 32.3±50.2% and 35.1±59.8%, respectively, higher at 20° compared to 110°. The average torque generated by train stimulations at 20° was 4.5±29.2% greater compared to 110°. However, the average torque generated by twitch stimulations at at 20° was 32.5±45.2% smaller compared to 110°.

IV. DISCUSSION

In this paper, we demonstrate the utility of combining electrical stimulation and A-Mode ultrasound to monitor stimulation-induced changes in muscle deformation, offering the potential for a low profile, wearable, and continuous method for measuring muscle fatigue. Our findings reveal that stimulation-induced, ultrasound-derived muscle deformation metrics can accurately track the progression of muscle fatigue before, during, and after strenuous activity. This approach overcomes limitations of traditional clinical assessments, which primarily rely on discrete, volitional force measurements before and after a fatiguing activity, by circumventing

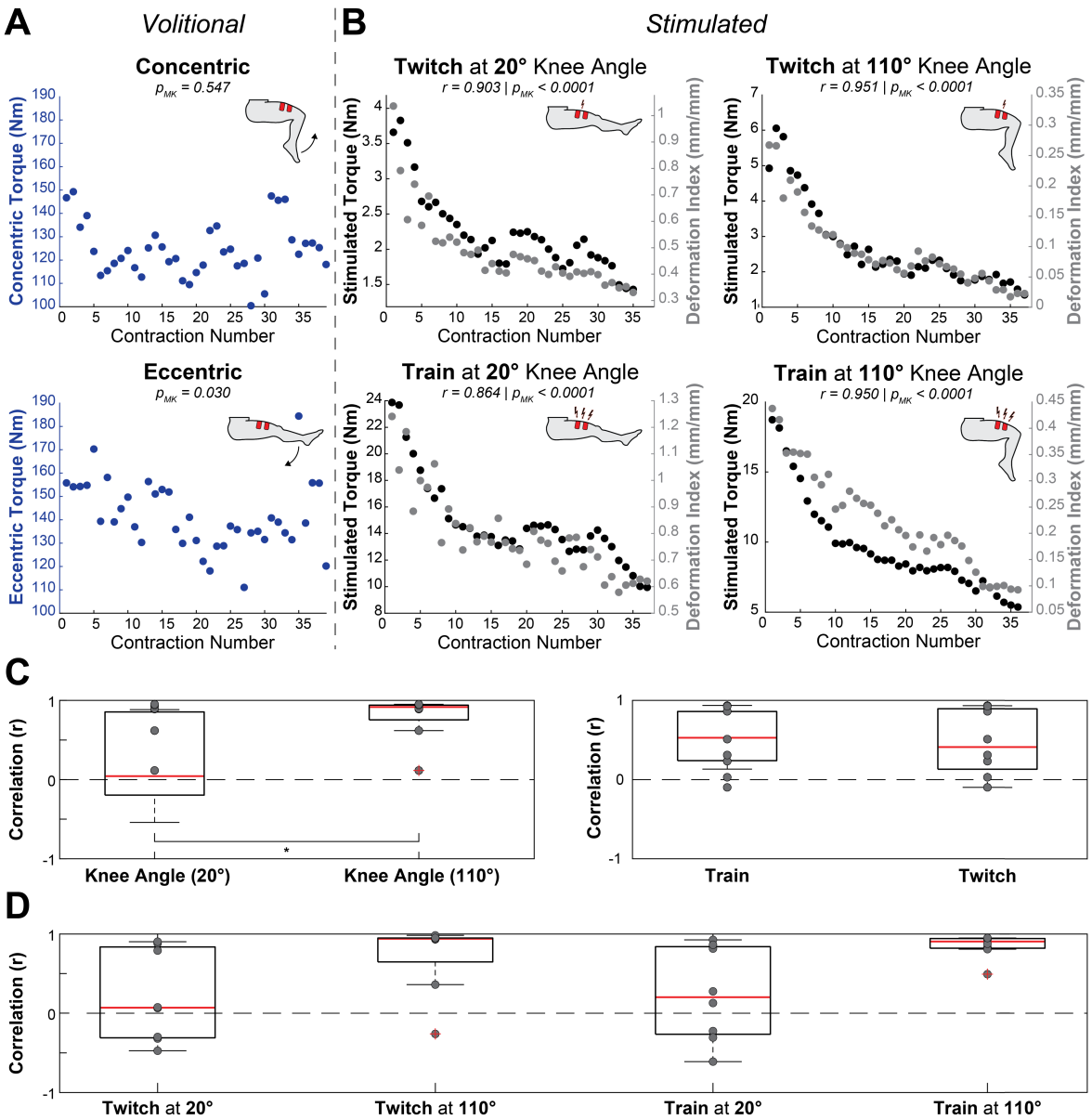

Fig. 4. Overview of results from the fatiguing protocol. (A) Scatter plot of maximum volitional concentric and eccentric torque per contraction for a single participant, with the Mann-Kendall p-values listed. (B) Scatter plot of stimulated torque and deformation index per contraction expanded by knee angle and stimulation type for the same participant, with the Mann-Kendall p-values and correlation values between stimulated torque and deformation index listed. (C) Box plot depicting correlation between stimulated torque and deformation index across stimulation types (left) and knee angles (right) for all participants. (D) Box plot depicting correlation between stimulated torque and deformation index across stimulation types and knee angles for all participants (n = 8). *Indicates statistically significant mean differences between conditions (determined via linear mixed model, $p < 0.05$).

the need for a force measurement apparatus and the variability associated with volitional control [12]. The direct activation of muscles with stimulation is particularly advantageous for continuous fatigue monitoring, where motivation and concentration can waver. Additionally, this approach does not require calibration, as we are looking at relative changes over time in response to a known stimulation input, and thus consistent muscle activation.

Standard clinical assessments of fatigue compare volitionally-generated joint torque before and after a fatiguing exercise, with a decrease in joint torque indicating fatigue. In our study, all participants exhibited a significant decrease in maximum volitionally-generated isometric torque after the fatiguing protocol (mean MVIC reduction of 32.1%, Fig. 3D and E), confirming fatigue. This decrease was paralleled by reductions in EMG-measured RMS voltage, although no significant changes were observed in MDF. Alongside the volitional reductions in torque, there was a significant decrease in stimulated torque following the fatiguing protocol, with corresponding reductions in the ultrasound-derived deformation index, regardless of the stimulation intensity used (Fig. 3F and G, and Table I). These ultrasound-derived results are consistent with prior benchtop studies using TMG, which reported similar reductions in elicited muscle belly radial displacement following dynamic volitional fatiguing protocols [11], [70], [71], [72], [73]. These

findings highlight the sensitivity of our stimulation-induced, ultrasound-derived deformation index in detecting muscle fatigue.

To demonstrate the capability of our combined electrical stimulation and A-mode ultrasound approach for tracking muscle fatigue (i.e., not comparing pre-post torque generation), we analyzed the correlation between stimulated torque and the ultrasound-derived deformation index throughout the fatiguing protocol. We found a robust correlation ($r = 0.85\pm0.15$) between ground-truth stimulated torque and the ultrasound-derived deformation index when delivering train stimulation at a knee angle of 110°. This correlation was stronger than those observed between EMG-derived metrics and volitionally-generated concentric and eccentric torques (concentric RMS: 0.56±0.3, MDF: 0.29±0.35; eccentric RMS: 0.61±0.32, MDF: 0.02±0.31) during the fatiguing protocol. Although a direct comparison with existing literature is not possible due to the absence of studies comparing ultrasound-measured deformation to stimulation-generated torque during dynamic volitional fatiguing protocols, a recent study did find a correlation of 0.89±0.25 between B-mode ultrasound echogenicity of the tibialis anterior and functional electrical stimulation-induced fatigue during isotonic dorsiflexion of the ankle [38]. The correlation between the deformation index and stimulated torque aligns well with such measurements from prior research. Ultimately, continuous monitoring of muscle fatigue could enable real-time adjustments during rehabilitation and training sessions, compared to traditional, discrete pre-post assessments, such as those conducted on a dynamometer or using TMG.

Standard muscle fatigue assessment protocols have high inherent variability as they rely on subjective maximum voluntary contractions [9], [10], [12]. To address this, traditional approaches often require three to five MVCs. However, this approach can inadvertently confound results by inducing fatigue through the testing process itself. Additionally, MVC testing can be impractical for certain populations, such as those recovering from injury or surgery, who are physically unable to perform at maximum effort without risking re-injury. Our findings highlight the inherent variability of volitional testing: although MVIC torque showed significant reductions post-exercise, the volitionally-generated torque during the dynamic concentric and eccentric phases of the fatiguing protocol varied considerably among participants (Table II). Despite all eight participants showing significant fatigue in pre-post comparisons, only two participants exhibited significant monotonic trends (p_{MK}<0.01) in their volitionally-generated concentric and eccentric torque during the protocol, according to the Mann-Kendall test results. This variability can compromise EMG's ability to track fatigue, as evidenced by the comparatively weak to moderate correlations observed between EMG RMS, EMG MDF, and isokinetic torque. This underscores the challenges of using EMG for fatigue monitoring during dynamic activities where volitional effort may vary [10]. By directly activating the muscle with a known and consistent input with ES, we demonstrate how we can limit neurological confounds and more accurately measure the peripheral changes to the muscle's force-generating mechanisms. In contrast to the volitionally-generated torque during the isokinetic contractions, stimulated torque at flexed and extended knee angles showed significant Mann-Kendall trends in nearly all participants (except one participant at extended knee angles). The enhanced consistency and reliability of stimulated torque measurements highlight the potential utility of stimulation in clinical and experimental settings, particularly in scenarios requiring precise and repeatable measurements, such as fatigue assessment. In addition, the electrically-induced stimulations in our study elicited no more than 10% of an individual's maximum force output, potentially making fatigue monitoring safer and more accessible for groups traditionally excluded from MVC assessments.

At the highest level, fatigue occurs because force-generating contractile proteins become impaired [74]. As fatigue develops, there is a decrease in the force-generating capacity of a muscle that is associated with changes in its deformation [3]. This reduction in force is due to various factors, including the depletion of energy stores, accumulation of metabolic byproducts (e.g., lactic acid), and impairments in the excitation-contraction coupling process, which affect muscle fibers' ability to contract efficiently [19], [74], [75]. We know that as fatigue progresses, there is a parallel reduction in overall muscle deformation and contractility [76], [77], [78]. During strenuous activity, the accumulation of metabolic byproducts impairs the interaction between actin and myosin, reducing the muscle's ability to contract forcefully and thus decreasing muscle deformation [3]. Additionally, a reduction in calcium release during prolonged activity weakens contractions can further limit the muscle's capacity to deform, which mechanically reflects its diminishing contractile power. Parallel to a reduction in force and deformation, muscle swelling can also occur due to an increase in blood flow to the area. As the body attempts to provide more oxygen and remove waste products, the accumulation of metabolic byproducts draws water into the muscle tissue, causing edema. In addition, during intense exercise, there could be microscopic damage to muscle fibers, leading to an inflammatory response that further contributes to swelling [66]. With our combined ES + SET approach, we are able to independently measure both the transient reductions in the force-generating capacity (as elicited deformation; ΔMT) as well as longer-time-scale changes in muscle swelling (by tracking baseline thickness changes; MT_0). The deformation index combines both signals to provide a single, holistic view of muscle architectural changes during fatigue.

To further validate the efficacy of the combined ES + SET approach, we examined the impact of joint angle on the correlation between muscle deformation and torque during fatigue. Our findings revealed that correlations between muscle deformation and stimulated torque during fatigue varied significantly with knee angle, with significantly higher correlations observed at a 110° knee angle ($r = 0.79\pm0.33$) compared to those at 20° ($r = 0.22\pm0.56$) (Fig. 4C and D). This variation is likely influenced by the muscle's force-length relationship, which describes how muscle force generation varies across the range of motion and has been shown to influence ultrasound [79] and TMG [80], [81]

measurements of deformation at different joint angles, as well as the rate of fatigue development [18], [82]. For the knee extensors, longer muscle lengths and increased pre-tension at a flexed knee angle (110°) led to more consistent deformation measurements, while shorter muscle lengths and less pre-tension at extended knee angles (20°) resulted in more deformation with increased variability [80], [81]. Variability in deformation is in part due to musculotendon coupling, which results in muscle translation during joint rotation, affecting the positioning of the muscle relative to the skin surface, stimulation electrodes, and ultrasound transducer, independent of force generation [33], [36], [49], [83]. These results highlight the importance of considering joint angle in the practical implementation of wearable systems for continuous fatigue monitoring, particularly when estimating fatigue during dynamic activities where the timing of stimulation should account for the current joint angle.

In addition to exploring joint angles, we also investigated the impact of different stimulation types on our approach. We assessed the correlation between stimulated torque and the ultrasound-derived deformation index during fatigue, and found no significant effect of stimulation type (train: $r = 0.54 \pm 0.52$; twitch: $r = 0.46 \pm 0.57$) (Fig. 4C and D). These findings align with results from the pre-post fatigue evaluation, which revealed a similar percent reduction of the ultrasound-derived deformation index between twitch and train stimulations. The lack of significant differences between stimulation types is notable, given that train stimulations elicited, on average, 59.2% more torque and 47.1% more thickness change than twitch stimulations during isometric contractions. This consistency across stimulation types suggests that lower levels of stimulation may be sufficient for effective fatigue monitoring. Implementing lower stimulation levels can enhance comfort, minimize the risk of inducing additional fatigue, and avoid unintended joint movements due to excessive stimulation. Consequently, this could improve the feasibility and tolerability of continuous fatigue monitoring systems in real-world settings, while maintaining measurement accuracy. Future work is needed to identify the lowest stimulation intensity that can still yield accurate and reliable estimates of fatigue.

True adoption of an approach for continuous monitoring of fatigue in unconstrained environments will require further research. Although this work demonstrated strong correlations between the stimulation-induced torque and the ultrasound-derived deformation index during fatigue, the generalizability of these findings is limited to semi-constrained, isokinetic movements on a dynamometer. Additionally, all participants in this study were young, healthy adults who self-reported as moderate to highly active individuals. Factors such as subcutaneous tissue thickness, which have been shown to modulate the TMG response [84], might vary significantly in other populations. Future research should explore how these results might differ in less active, aging, or clinical populations where variations in physiological characteristics such as subcutaneous tissue could influence outcomes. Also, although our approach demonstrates the potential for wearability and real-time implementation [49], currently the deformation index calculation was performed offline, in post-processing. Additionally, because current technology does not allow for the non-invasive measurement of force from individual muscles [30], this work utilized a dynamometer to measure overall knee extension torque, which results from the combined effort of multiple knee extensors. Consequently, we measured the bulk deformation of the rectus femoris and vastus intermedius in response to stimulation. Although this approach may limit interpretability regarding muscle specificity, A-mode ultrasound has proven capable of tracking individual muscle thickness changes [49]. Finally, we noted joint angle-specific changes in muscle deformation with stimulation. At 20°, the knee extensor compartment increased in thickness in response to stimulation for all participants; however, at 110°, it decreased for 7 out of 8 participants. This may be due to muscle deformation occurring perpendicular to the imaging plane at more flexed angles (i.e., the muscle expands in width, perpendicular to the skin surface, thus registering as a decrease in thickness when assessed with our A-Mode system). Additionally, although fatigue in this study was induced during dynamic contractions, deformation index measurements were taken under static conditions at each end of the ROM. As stimulation-induced deformation is known to differ from deformation caused by volitional contraction and joint movement [85], understanding these dynamics will be crucial for accurately interpreting deformation signals in dynamic applications where joint angles continuously vary.

Our study introduces an approach for semi-continuous fatigue monitoring by tracking changes in electrical stimulation-induced muscle deformation with A-Mode ultrasound. Our results demonstrate how this combined methodology can provide highly correlated measures of muscle fatigue when compared to stimulated torque during a dynamic knee extension fatiguing protocol. By directly activating muscle with stimulation, this approach could also be used to track muscle fatigue in populations that historically could not be measured with traditional methods due to minimal muscle activity or volitional control (e.g., multiple sclerosis or stroke). Finally, although in this study we only measured deformation in response to stimulation delivered to resting muscle, stimulating during volitional contractions could provide deeper insights into the central mechanisms of fatigue [86].

Acknowledgment

The authors would like to thank David Adam Quirk, Umut S. Civici, Philipp Arens, and Mollie Ebeling for advice on illustrations and statistical analysis, as well as the Wyss Institute Clinical Research Team for their help with the development of the study protocol.

References

[1] P. A. Merton, "Voluntary strength and fatigue," *J. Physiol.*, vol. 123, no. 3, pp. 553–564, Mar. 1954.

[2] S. A. Binder-Macleod and L. Snyder-Mackler, "Muscle fatigue: Clinical implications for fatigue assessment and neuromuscular electrical stimulation," *Phys. Therapy*, vol. 73, no. 12, pp. 902–910, Dec. 1993.

[3] N. K. Vøllestad, "Measurement of human muscle fatigue," *J. Neurosci. Methods*, vol. 74, no. 2, pp. 219–227, Jun. 1997.

[4] J. F. Tornero-Aguilera, J. Jimenez-Morcillo, A. Rubio-Zarapuz, and V. J. Clemente-Suárez, "Central and peripheral fatigue in physical exercise explained: A narrative review," *Int. J. Environ. Res. Public Health*, vol. 19, no. 7, p. 3909, Mar. 2022.

[5] B. Bigland-Ritchie, F. Furbush, and J. J. Woods, "Fatigue of intermittent submaximal voluntary contractions: Central and peripheral factors," *J. Appl. Physiol.*, vol. 61, no. 2, pp. 421–429, Aug. 1986.

[6] P. Kannus, "Isokinetic evaluation of muscular performance," *Int. J. Sports Med.*, vol. 15, no. S 1, pp. S11–S18, Jan. 1994.

[7] N. A. Maffiuletti, M. Bizzini, K. Desbrosses, N. Babault, and U. Munzinger, "Reliability of knee extension and flexion measurements using the con-trex isokinetic dynamometer," *Clin. Physiol. Funct. Imag.*, vol. 27, no. 6, pp. 346–353, Nov. 2007.

[8] P. J. McNair, J. Depledge, M. Brettkelly, and S. N. Stanley, "Verbal encouragement: Effects on maximum effort voluntary muscle: Action," *Brit. J. Sports Med.*, vol. 30, no. 3, pp. 243–245, Sep. 1996.

[9] A. Burden and R. Bartlett, "Normalisation of EMG amplitude: An evaluation and comparison of old and new methods," *Med. Eng. Phys.*, vol. 21, no. 4, pp. 247–257, May 1999.

[10] A. Burden, "How should we normalize electromyograms obtained from healthy participants? What we have learned from over 25years of research," *J. Electromyogr. Kinesiol.*, vol. 20, no. 6, pp. 1023–1035, Dec. 2010.

[11] M. Kalc, K. Puš, A. Paravlic, J. Urbanc, and B. Šimunič, "Diagnostic accuracy of tensiomyography parameters for monitoring peripheral neuromuscular fatigue," *J. Electromyogr. Kinesiol.*, vol. 70, Jun. 2023, Art. no. 102775.

[12] H. Norasi, J. Koenig, and G. A. Mirka, "Development and assessment of a method to estimate the value of a maximum voluntary isometric contraction electromyogram from submaximal electromyographic data," *J. Appl. Biomech.*, vol. 38, no. 2, pp. 76–83, Apr. 2022.

[13] L. N. Awad, H. Hsiao, and S. A. Binder-Macleod, "Central drive to the paretic ankle plantarflexors affects the relationship between propulsion and walking speed after stroke," *J. Neurolog. Phys. Therapy*, vol. 44, no. 1, pp. 42–48, 2020.

[14] A. N. Collimore et al., "A portable, neurostimulation-integrated, force measurement platform for the clinical assessment of plantarflexor central drive," *Bioengineering*, vol. 11, no. 2, p. 137, Jan. 2024.

[15] S. L. Halson, "Monitoring training load to understand fatigue in athletes," *Sports Med.*, vol. 44, no. S2, pp. 139–147, Nov. 2014.

[16] D. R. Seshadri et al., "Wearable sensors for monitoring the internal and external workload of the athlete," *NPJ Digit. Med.*, vol. 2, no. 1, p. 71, Jul. 2019.

[17] R. Lepers, C. Hausswirth, N. Maffiuletti, J. Brisswalter, and J. Van Hoecke, "Evidence of neuromuscular fatigue after prolonged cycling exercise," *Med. Sci. Sports Exerc.*, vol. 32, no. 11, pp. 1880–1886, Nov. 2000.

[18] J. Pethick, S. L. Winter, and M. Burnley, "Fatigue-induced changes in knee-extensor torque complexity and muscle metabolic rate are dependent on joint angle," *Eur. J. Appl. Physiol.*, vol. 121, no. 11, pp. 3117–3131, Nov. 2021.

[19] J. Finsterer, "Biomarkers of peripheral muscle fatigue during exercise," *BMC Musculoskeletal Disorders*, vol. 13, no. 1, p. 218, Dec. 2012.

[20] S. R. Perry-Rana, T. J. Housh, G. O. Johnson, A. J. Bull, J. M. Berning, and J. T. Cramer, "MMG and EMG responses during fatiguing isokinetic muscle contractions at different velocities," *Muscle Nerve*, vol. 26, no. 3, pp. 367–373, Sep. 2002.

[21] J. Sun, G. Liu, Y. Sun, K. Lin, Z. Zhou, and J. Cai, "Application of surface electromyography in exercise fatigue: A review," *Frontiers Syst. Neurosci.*, vol. 16, Aug. 2022, Art. no. 893275.

[22] M. A. Islam, K. Sundaraj, R. B. Ahmad, and N. U. Ahamed, "Mechanomyogram for muscle function assessment: A review," *PLoS ONE*, vol. 8, no. 3, Mar. 2013, Art. no. e58902.

[23] J. Naeem, N. A. Hamzaid, M. A. Islam, A. W. Azman, and M. Bijak, "Mechanomyography-based muscle fatigue detection during electrically elicited cycling in patients with spinal cord injury," *Med. Biol. Eng. Comput.*, vol. 57, no. 6, pp. 1199–1211, Jun. 2019.

[24] Y. Yoshitake, H. Ue, M. Miyazaki, and T. Moritani, "Assessment of lower-back muscle fatigue using electromyography, mechanomyography, and near-infrared spectroscopy," *Eur. J. Appl. Physiol.*, vol. 84, no. 3, pp. 174–179, 2001.

[25] W. Guo, X. Sheng, and X. Zhu, "Assessment of muscle fatigue based on motor unit firing, muscular vibration and oxygenation via hybrid mini-grid sEMG, MMG, and NIRS sensing," *IEEE Trans. Instrum. Meas.*, vol. 71, pp. 1–10, 2022.

[26] N. Li et al., "Non-invasive techniques for muscle fatigue monitoring: A comprehensive survey," *ACM Comput. Surv.*, vol. 56, no. 9, pp. 1–40, Oct. 2024.

[27] M. A. Islam, K. Sundaraj, R. B. Ahmad, N. U. Ahamed, and M. A. Ali, "Mechanomyography sensor development, related signal processing, and applications: A systematic review," *IEEE Sensors J.*, vol. 13, no. 7, pp. 2499–2516, Jul. 2013.

[28] N. A. Dimitrova and G. V. Dimitrov, "Interpretation of EMG changes with fatigue: Facts, pitfalls, and fallacies," *J. Electromyogr. Kinesiol.*, vol. 13, no. 1, pp. 13–36, Feb. 2003.

[29] I. Campanini, C. Disselhorst-Klug, W. Z. Rymer, and R. Merletti, "Surface EMG in clinical assessment and neurorehabilitation: Barriers limiting its use," *Frontiers Neurol.*, vol. 11, p. 934, Sep. 2020.

[30] T. J. Roberts and A. M. Gabaldon, "Interpreting muscle function from EMG: Lessons learned from direct measurements of muscle force," *Integrative Comparative Biol.*, vol. 48, no. 2, pp. 312–320, Jun. 2008.

[31] L. A. Hallock, "Muscle deformation correlates with output force during isometric contraction," in *Proc. 8th IEEE RAS/EMBS Int. Conf. Biomed. Robot. Biomechatronics*, Nov. 2020, pp. 1188–1195.

[32] S. Đorđević, S. Tomažič, M. Narici, R. Pišot, and A. Meglič, "In-vivo measurement of muscle tension: Dynamic properties of the MC sensor during isometric muscle contraction," *Sensors*, vol. 14, no. 9, pp. 17848–17863, Sep. 2014.

[33] J. T. Alvarez, A. de Marcillac, Y. Jin, L. F. Gerez, O. A. Araromi, and C. J. Walsh, "Surface-level muscle deformation as a correlate for joint torque," *Adv. Mater. Technol.*, vol. 9, no. 15, pp. 1–10, Aug. 2024.

[34] J. Shi, Z. Yong-Ping, H. Qing-Hua, and X. Chen, "Continuous monitoring of sonomyography, electromyography and torque generated by normal upper arm muscles during isometric contraction: Sonomyography assessment for arm muscles," *IEEE Trans. Biomed. Eng.*, vol. 55, no. 3, pp. 1191–1198, Mar. 2008.

[35] X. Chen, Y.-P. Zheng, J.-Y. Guo, Z. Zhu, S.-C. Chan, and Z. Zhang, "Sonomyographic responses during voluntary isometric ramp contraction of the human rectus femoris muscle," *Eur. J. Appl. Physiol.*, vol. 112, no. 7, pp. 2603–2614, Jul. 2012.

[36] L. A. Hallock, A. Kato, and R. Bajcsy, "Empirical quantification and modeling of muscle deformation: Toward ultrasound-driven assistive device control," in *Proc. IEEE Int. Conf. Robot. Autom. (ICRA)*, Jun. 2018, pp. 1825–1832.

[37] Q. Zhang, A. Iyer, K. Lambeth, K. Kim, and N. Sharma, "Ultrasound echogenicity-based assessment of muscle fatigue during functional electrical stimulation," in *Proc. 43rd Annu. Int. Conf. IEEE Eng. Med. Biol. Soc. (EMBC)*, Dec. 2021, pp. 5948–5952.

[38] Q. Zhang, A. Iyer, K. Lambeth, K. Kim, and N. Sharma, "Ultrasound echogenicity as an indicator of muscle fatigue during functional electrical stimulation," *Sensors*, vol. 22, no. 1, p. 335, Jan. 2022.

[39] Q. Zhang, K. Lambeth, A. Iyer, Z. Sun, and N. Sharma, "Ultrasound imaging-based closed-loop control of functional electrical stimulation for drop foot correction," *IEEE Trans. Control Syst. Technol.*, vol. 31, no. 3, pp. 989–1005, May 2023.

[40] R. S. Witte, K. Kim, B. J. Martin, and M. O'Donnell, "Effect of fatigue on muscle elasticity in the human forearm using ultrasound strain imaging," in *Proc. Int. Conf. IEEE Eng. Med. Biol. Soc.*, Aug. 2006, pp. 4490–4493.

[41] Z. Sheng, N. Sharma, and K. Kim, "Quantitative assessment of changes in muscle contractility due to fatigue during NMES: An ultrasound imaging approach," *IEEE Trans. Biomed. Eng.*, vol. 67, no. 3, pp. 832–841, Mar. 2020.

[42] Z. Sheng, N. Sharma, and K. Kim, "Ultra-high-frame-rate ultrasound monitoring of muscle contractility changes due to neuromuscular electrical stimulation," *Ann. Biomed. Eng.*, vol. 49, no. 1, pp. 262–275, Jan. 2021.

[43] P. Li, X. Yang, G. Yin, and J. Guo, "Skeletal muscle fatigue state evaluation with ultrasound image entropy," *Ultrasonic Imag.*, vol. 42, no. 6, pp. 235–244, 2020.

[44] J. Shi, Y.-P. Zheng, X. Chen, and Q.-H. Huang, "Assessment of muscle fatigue using sonomyography: Muscle thickness change detected from ultrasound images," *Med. Eng. Phys.*, vol. 29, no. 4, pp. 472–479, 2007.

[45] T. E. Kuehne, N. Yitzchaki, M. B. Jessee, B. S. Graves, and S. L. Buckner, "A comparison of acute changes in muscle thickness between A-mode and B-mode ultrasound," *Physiolog. Meas.*, vol. 40, no. 11, Dec. 2019, Art. no. 115004.

[46] I. AlMohimeed and Y. Ono, "Ultrasound measurement of skeletal muscle contractile parameters using flexible and wearable single-element ultrasonic sensor," *Sensors*, vol. 20, no. 13, p. 3616, Jun. 2020.

[47] X. Xue, S. Moon, V. Ganesh, B. Zhang, N. Sharma, and X. Jiang, "Advancing quadriceps muscle monitoring: Wearable A-mode ultrasound and machine learning classification for accurate estimation of muscle states," in *Proc. IEEE Int. Ultrason. Symp. (IUS)*, Sep. 2023, pp. 1–4.

[48] Q. Zengyu et al., "A simultaneous gesture classification and force estimation strategy based on wearable A-mode ultrasound and cascade model," *IEEE Trans. Neural Syst. Rehabil. Eng.*, vol. 30, pp. 2301–2311, 2022.

[49] Y. Jin et al., "Estimation of joint torque in dynamic activities using wearable A-mode ultrasound," *Nature Commun.*, vol. 15, no. 1, p. 5756, Jul. 2024.

[50] X. Yang, X. Sun, D. Zhou, Y. Li, and H. Liu, "Towards wearable A-mode ultrasound sensing for real-time finger motion recognition," *IEEE Trans. Neural Syst. Rehabil. Eng.*, vol. 26, no. 6, pp. 1199–1208, Jun. 2018.

[51] L. Brausch, H. Hewener, and P. Lukowicz, "Classifying muscle states with one-dimensional radio-frequency signals from single element ultrasound transducers," *Sensors*, vol. 22, no. 7, p. 2789, Apr. 2022.

[52] X. Sun, Y. Li, and H. Liu, "Muscle fatigue assessment using one-channel single-element ultrasound transducer," in *Proc. 8th Int. IEEE/EMBS Conf. Neural Eng. (NER)*, May 2017, pp. 122–125.

[53] M. Qu et al., "Continuously monitoring of muscle fatigue based on a wearable micromachined ultrasonic transducer probe," *Sens. Actuators A, Phys.*, vol. 365, Jan. 2024, Art. no. 114892.

[54] B. Bigland-Ritchie and J. J. Woods, "Changes in muscle contractile properties and neural control during human muscular fatigue," *Muscle Nerve*, vol. 7, no. 9, pp. 691–699, Dec. 1984.

[55] A. Werkhausen, Ø. Gløersen, A. Nordez, G. Paulsen, J. Bojsen-Møller, and O. R. Seynnes, "Linking muscle architecture and function in vivo: Conceptual or methodological limitations?" *PeerJ*, vol. 11, Apr. 2023, Art. no. e15194.

[56] L. J. Macgregor, A. M. Hunter, C. Orizio, M. M. Fairweather, and M. Ditroilo, "Assessment of skeletal muscle contractile properties by radial displacement: The case for tensiomyography," *Sports Med.*, vol. 48, no. 7, pp. 1607–1620, Mar. 2018.

[57] E. Cè, S. Longo, E. Limonta, G. Coratella, S. Rampichini, and F. Esposito, "Peripheral fatigue: New mechanistic insights from recent technologies," *Eur. J. Appl. Physiol.*, vol. 120, no. 1, pp. 17–39, Jan. 2020.

[58] M. J. Hambly, A. C. C. de Sousa, and C. Pizzolato, "Comparison of filtering methods for real-time extraction of the volitional EMG component in electrically stimulated muscles," *Biomed. Signal Process. Control*, vol. 87, Jan. 2024, Art. no. 105471.

[59] R. Uwamahoro, K. Sundaraj, and I. D. Subramaniam, "Assessment of muscle activity using electrical stimulation and mechanomyography: A systematic review," *Biomed. Eng. OnLine*, vol. 20, no. 1, p. 1, Dec. 2021.

[60] M. O. Ibitoye, N. A. Hamzaid, J. M. Zuniga, and A. K. A. Wahab, "Mechanomyography and muscle function assessment: A review of current state and prospects," *Clin. Biomech.*, vol. 29, no. 6, pp. 691–704, 2014.

[61] R. J. Downey, M. Merad, E. J. Gonzalez, and W. E. Dixon, "The time-varying nature of electromechanical delay and muscle control effectiveness in response to stimulation-induced fatigue," *IEEE Trans. Neural Syst. Rehabil. Eng.*, vol. 25, no. 9, pp. 1397–1408, Sep. 2017.

[62] W. M. Grill and J. T. Mortimer, "The effect of stimulus pulse duration on selectivity of neural stimulation," *IEEE Trans. Biomed. Eng.*, vol. 43, no. 2, pp. 161–166, Feb. 1996.

[63] H. J. Hermens, B. Freriks, C. Disselhorst-Klug, and G. Rau, "Development of recommendations for SEMG sensors and sensor placement procedures," *J. Electromyogr. Kinesiol.*, vol. 10, no. 5, pp. 361–374, 2000.

[64] C. J. De Luca, L. Donald Gilmore, M. Kuznetsov, and S. H. Roy, "Filtering the surface EMG signal: Movement artifact and baseline noise contamination," *J. Biomechanics*, vol. 43, no. 8, pp. 1573–1579, May 2010.

[65] A. A. Vandervoort, J. Quinlan, and A. J. McComas, "Twitch potentiation after voluntary contraction," *Experim. Neurol.*, vol. 81, no. 1, pp. 141–152, Jul. 1983.

[66] T. Yasuda, K. Fukumura, H. Iida, and T. Nakajima, "Effect of low-load resistance exercise with and without blood flow restriction to volitional fatigue on muscle swelling," *Eur. J. Appl. Physiol.*, vol. 115, no. 5, pp. 919–926, May 2015.

[67] K. T. Ebersole, T. J. Housh, G. O. Johnson, T. K. Evetovich, D. B. Smith, and S. R. Perry, "MMG and EMG responses of the superficial quadriceps femoris muscles," *J. Electromyogr. Kinesiol.*, vol. 9, no. 3, pp. 219–227, Apr. 1999.

[68] R. K. Pearson, Y. Neuvo, J. Astola, and M. Gabbouj, "Generalized Hampel filters," *EURASIP J. Adv. Signal Process.*, vol. 2016, no. 1, p. 87, Dec. 2016.

[69] M. Gocic and S. Trajkovic, "Analysis of changes in meteorological variables using Mann–Kendall and Sen's slope estimator statistical tests in Serbia," *Global Planet. Change*, vol. 100, pp. 172–182, Jan. 2013.

[70] L. Carrasco, B. Sañudo, M. de Hoyo, F. Pradas, and M. E. Da Silva, "Effectiveness of low-frequency vibration recovery method on blood lactate removal, muscle contractile properties and on time to exhaustion during cycling at VO2max power output," *Eur. J. Appl. Physiol.*, vol. 111, no. 9, pp. 2271–2279, Sep. 2011.

[71] J. M. García-Manso, D. Rodríguez-Ruiz, D. Rodríguez-Matoso, Y. de Saa, S. Sarmiento, and M. Quiroga, "Assessment of muscle fatigue after an ultra-endurance triathlon using tensiomyography (TMG)," *J. Sports Sci.*, vol. 29, no. 6, pp. 619–625, Mar. 2011.

[72] J. M. García-Manso et al., "Effect of high-load and high-volume resistance exercise on the tensiomyographic twitch response of biceps brachii," *J. Electromyogr. Kinesiol.*, vol. 22, no. 4, pp. 612–619, Aug. 2012.

[73] L. J. Macgregor, M. Ditroilo, I. J. Smith, M. M. Fairweather, and A. M. Hunter, "Reduced radial displacement of the gastrocnemius medialis muscle after electrically elicited fatigue," *J. Sport Rehabil.*, vol. 25, no. 3, pp. 241–247, Aug. 2016.

[74] R. M. Enoka and J. Duchateau, "Muscle fatigue: What, why and how it influences muscle function," *J. Physiol.*, vol. 586, no. 1, pp. 11–23, Jan. 2008.

[75] J.-J. Wan, Z. Qin, P.-Y. Wang, Y. Sun, and X. Liu, "Muscle fatigue: General understanding and treatment," *Experim. Mol. Med.*, vol. 49, no. 10, p. e384, Oct. 2017.

[76] R. S. Witte, D. E. Dow, R. Olafsson, Y. Shi, and M. O'Donnell, "High resolution ultrasound imaging of skeletal muscle dynamics and effects of fatigue," in *Proc. IEEE Ultrason. Symp.,*, vol. 1, Jun. 2004, pp. 764–767.

[77] R. Martín-San Agustín, F. Medina-Mirapeix, J. Casaña-Granell, J. A. García-Vidal, C. Lillo-Navarro, and J. C. Benítez-Martínez, "Tensiomyographical responsiveness to peripheral fatigue in quadriceps femoris," *PeerJ*, vol. 8, p. e8674, Feb. 2020.

[78] J. A. Majdi, S. A. Acuña, P. V. Chitnis, and S. Sikdar, "Toward a wearable monitor of local muscle fatigue during electrical muscle stimulation using tissue Doppler imaging," *Wearable Technol.*, vol. 3, p. e16, Jul. 2022, doi: 10.1017/wtc.2022.10. [Online]. Available: https://www.cambridge.org/core/journals/wearable-technologies/article/toward-a-wearable-monitor-of-local-muscle-fatigue-during-electrical-muscle-stimulation-using-tissue-doppler-imaging/4ADA49B3A98D245E222D5CCFDE1F180D

[79] S. Fitch and A. McComas, "Influence of human muscle length on fatigue," *J. Physiol.*, vol. 362, no. 1, pp. 205–213, May 1985.

[80] M. Ditroilo, A. M. Hunter, S. Haslam, and G. De Vito, "The effectiveness of two novel techniques in establishing the mechanical and contractile responses of biceps femoris," *Physiolog. Meas.*, vol. 32, no. 8, pp. 1315–1326, Aug. 2011.

[81] C. Latella, C. V. Ruas, R. N. O. Mesquita, K. Nosaka, and J. L. Taylor, "Test-retest reliability of elbow flexor contraction characteristics with tensiomyography for different elbow joint angles," *J. Electromyogr. Kinesiol.*, vol. 45, pp. 26–32, Apr. 2019.

[82] C. J. de Ruiter, M. D. de Boer, M. Spanjaard, and A. de Haan, "Knee angle-dependent oxygen consumption during isometric contractions of the knee extensors determined with near-infrared spectroscopy," *J. Appl. Physiol.*, vol. 99, no. 2, pp. 579–586, Aug. 2005.

[83] J. T. Alvarez et al., "Towards soft wearable strain sensors for muscle activity monitoring," *IEEE Trans. Neural Syst. Rehabil. Eng.*, vol. 30, pp. 2198–2206, 2022.

[84] C. Calvo-Lobo, I. Díez-Vega, M. García-Mateos, J. J. Molina-Martín, G. Díaz-Ureña, and D. Rodríguez-Sanz, "Relationship of the skin and subcutaneous tissue thickness in the tensiomyography response: A novel ultrasound observational study," *Revista da Associação Médica Brasileira*, vol. 64, no. 6, pp. 549–553, Jun. 2018.

[85] S. Qiu et al., "Sonomyography analysis on thickness of skeletal muscle during dynamic contraction induced by neuromuscular electrical stimulation: A pilot study," *IEEE Trans. Neural Syst. Rehabil. Eng.*, vol. 25, no. 1, pp. 62–70, Jan. 2017.

[86] J. L. Taylor and S. C. Gandevia, "A comparison of central aspects of fatigue in submaximal and maximal voluntary contractions," *J. Appl. Physiol.*, vol. 104, no. 2, pp. 542–550, Feb. 2008.